Aurora Kinase Inhibitor PHA-739358 Suppresses Growth of Hepatocellular Carcinoma *In Vitro* and in a Xenograft Mouse Model[1]

Daniel Benten[*,2], Gunhild Keller[†,2], Alexander Quaas[‡], Jorg Schrader[*], Artur Gontarewicz[†], Stefan Balabanov[†], Melanie Braig[†], Henning Wege[*], Jurgen Moll[§], Ansgar W. Lohse[*] and Tim H. Brummendorf[†]

[*]I. Medizinische Klinik, Universitätsklinikum Hamburg-Eppendorf, Hamburg, Germany; [†]Universitäres Cancer Center Hamburg, Universitätsklinikum Hamburg-Eppendorf, Hamburg, Germany; [‡]Pathologisches Institut, Universitätsklinikum Hamburg-Eppendorf, Hamburg, Germany; [§]Nerviano Medical Sciences, Milan, Italy

Abstract

Patients with advanced stages of hepatocellular carcinoma (HCC) face a poor prognosis. Although encouraging clinical results have been obtained with multikinase inhibitor sorafenib, the development of improved therapeutic strategies for HCC remains an urgent goal. Aurora kinases are key regulators of the cell cycle, and their uncontrolled expression promotes aneuploidy and tumor development. In tissue microarray analyses, we detected aurora-A kinase expression in all of the examined 93 human HCC samples, whereas aurora-B kinase expression levels significantly correlated with the proliferation index of HCCs. In addition, two human HCC cell lines (Huh-7 and HepG2) were tested positive for aurora-A and -B and revealed Ser10 phosphorylation of histone H3, indicating an increased aurora-B kinase activity. The antiproliferative features of a novel aurora kinase inhibitor, PHA-739358, currently under investigation in phase 2 clinical trials for other solid tumors, were examined *in vitro* and *in vivo*. At concentrations exceeding 50 nM, PHA-739358 completely suppressed tumor cell proliferation in cell culture experiments and strongly decreased histone H3 phosphorylation. Cell cycle inhibition and endoreduplication were observed at 50 nM, whereas higher concentrations led to a complete G_2/M–phase arrest. *In vivo*, administration of PHA-739358 resulted in significant tumor growth inhibition at a well-tolerated dose. In combination with sorafenib, additive effects were observed. Remarkably, when tumors restarted to grow under sorafenib monotherapy, subsequent treatment with PHA-739358 induced tumor shrinkage by up to 81%. Thus, targeting aurora kinases with PHA-739358 is a promising therapeutic strategy administered alone or in combination with sorafenib for patients with advanced stages of HCC.

Neoplasia (2009) 11, 934–944

Introduction

Hepatocellular carcinoma (HCC) is the fifth most common malignancy worldwide and the fastest growing cause of cancer related death in men in the United States [1,2]. Although surveillance of patients with risk factors for HCC and development of locoregional treatment options have improved the outcome, curative treatment consisting of surgical resection, liver transplantation, or possibly radiofrequency ablation is applicable to only a minority with limited stage disease [3]. In intermediate, advanced or recurrent HCC, palliative cytotoxic chemotherapy is mostly ineffective, and thus, patients face a very poor prognosis. Until recently, chemoembolization was the only option to

decelerate tumor growth. On the basis of the results of a phase 3 study (SHARP), the multikinase inhibitor sorafenib was approved for treatment of unresectable HCC [4]. Sorafenib decreases tumor cell proliferation and inhibits tumor angiogenesis [5]. However, the effect is mostly moderate, and new therapeutic strategies for advanced HCC are mandatory.

Aurora kinases are key regulators of protein phosphorylation during mitosis [6]. These serine/threonine kinases interact with other proteins to control chromosome assembly and segregation. Aurora kinases consist of three members with differences in subcellular localization, kinetics of activation, and function [6]: aurora-A plays a role in centrosome maturation and spindle assembly, aurora-B regulates cytokinesis and chromosome cohesion as part of the spindle checkpoint, whereas Aurora-C is less well studied [7].

Overexpression of aurora-A and aurora-B has been described in several malignancies being associated with deregulation of chromosomal ploidy and a consecutive genetic instability. It has also been linked to pathophysiological and clinical parameters, such as p53 expression, tumor grading, lymph node invasion, disease progression, and survival [7]. Consequently, several small-molecule inhibitors have been developed showing antiproliferative effects on tumor cells in preclinical models. Recently, a highly effective aurora kinase inhibitor (AKI), PHA-739358, which was shown to inhibit all aurora kinases at nanomolar concentrations, has entered phase 2 clinical trials for patients with advanced stages of prostate cancer and hematological malignancies [8,9].

The role of aurora kinases in HCC has moved into the focus of preclinical research. Jeng et al. [10] demonstrated up-regulation of the aurora-A gene in HCC nodules compared with nontumorous liver tissues. In genome-wide gene expression profiles of surgically resected HCC, aurora-B gene expression was the only predictive factor for HCC recurrence [11], whereas the role of aurora kinase protein expression is largely unknown. First promising *in vitro* and *in vivo* results were yielded by VE-465, an AKI derivate of VX-680 [12]. To further elucidate aurora-A and -B kinase protein expression in HCC, we examined a large series of human HCC tissue samples with variable proliferative indices by immunohistochemistry. On the basis of the positive results, the antiproliferative features of AKI PHA-739358 were evaluated *in vitro* and *in vivo*, and possible therapeutic mechanisms were analyzed. Finally, we were able to demonstrate for the first time that combination therapy with sorafenib as well as treatment with PHA-739358 secondary to failure of sorafenib may be an applicable treatment strategy for patients with advanced stages of HCC.

Materials and Methods

Materials

Human-specific antibodies were used for the detection of Ki-67 (clone MIB-1); cytokeratin 18 (Dako, Hamburg, Germany); aurora-A and aurora-B (Abcam, Cambridge, UK); and phosphorylated histone H3(Ser10), caspase-3, and stathmin (Cell Signaling Technology, Danvers, MA). PHA-739358 was provided by Nerviano Medical Sciences Srl. (Milan, Italy). For cell culture experiments, a 10-µM stock solution in dimethyl sulfoxide (DMSO) was prepared. For *in vivo* experiments, an *in situ* salt was prepared by adding 1 µl 2N hydrochloric acid per milligram of PHA-739358 before dissolving in 5% dextrose at a concentration of 4.5 mg/ml. Sorafenib tosylate (purchased from LC Laboratories, Woburn, MA) was dissolved and handled as described in detail [13].

Tissue Microarray Construction

Tissue samples of surgically resected human HCCs or HCC nodules in explanted livers were fixed in 4% buffered formalin, embedded in paraffin, and used for tissue microarray (TMA) construction. Hematoxylin-eosin (H&E)–stained sections were made from selected primary tumor blocks (donor blocks) to define representative tumor regions. Tissue cylinders (0.6 mm in diameter) were punched from the representative region of the donor block using a semiautomatic tissue arrayer [14]. Control samples included cirrhotic liver parenchyma. Five-micrometer sections were cut for H&E staining and immunohistochemistry by use of the Paraffin Sectioning Aid System (Instrumentics, Hackensack, NJ).

TMA Immunohistochemistry and Analysis

Sections were deparaffinized by warming to 60°C for 1 hour followed by three 5-minute washes in xylene and dehydration in graded ethanol. For antigen retrieval, slides were immersed in 10 mM citrate buffer, pH 6.0, heated in a microwave oven for 15 minutes and cooled for 15 minutes at room temperature (RT). For immunostaining, sections were blocked in 3% H_2O_2 in methanol for 10 minutes and in bovine serum albumin in Tris-buffered saline containing 0.1% Tween-20 (TBS-T), pH 7.4, for 1 hour and incubated with primary antibodies in antibody diluent (Dako; Ki-67, clone MIB-1, 1:100; aurora-A, 1:100; aurora-B, 1:500) for 1 hour at RT. Sections were incubated with peroxidase-conjugated mouse- or rabbit-specific goat immunoglobulin G (IgG, 1:300; Real Envision HRP rabbit/mouse; Dako) for 30 minutes at RT with color development for 30 seconds to 10 minutes in diaminobenzidine (Dako). Tumor spots were considered uninterpretable if they had insufficient tumor cells or loss of tissue in the spot.

For morphometric analysis, a magnification of ×400 was used. The proliferation index was determined semiquantitatively by the fraction of Ki-67–stained cells (low [1%-5%], moderate [5%-30%], high [>30%]). Aurora-B staining was graded semiquantitatively from 0 (negative) to ++ (maximally positive staining intensity). Two observers (A.Q. and D.B.) graded tissues independently, and interobserver differences were reconciled by consensus.

Human HCC Cells and Culture

Huh-7 and HepG2 cells originating from well-differentiated human HCC tissues were maintained in Dulbecco's modified Eagle medium (Invitrogen, Karlsruhe, Germany), supplemented with 10% fetal calf serum, 100 U/ml penicillin, and 10 µg/ml streptomycin (Invitrogen) at 37°C in a 5% CO_2 atmosphere.

Cell Analysis and Immunostaining

Cells were seeded in 24-well flat-bottomed plates (Sarstedt, Numbrecht, Germany) at a density of 25×10^4 cells per well in 1 ml of their respective medium. Expression of aurora-A, aurora-B, and histone H3 phosphorylation was determined by immunostaining cells, fixing in methanol for 5 minutes, washing in phosphate-buffered saline (PBS), and being postfixed in 4% paraformaldehyde for 5 minutes (staining protocol described later). For the analysis of cell proliferation, increasing concentrations of PHA-739358 (dissolvent control, 5 nM to 5 µM) and/or sorafenib (dissolvent control, 1-10 µM) were added after 24 hours of cell culture. Approximately 48 to 120 hours later, the number of viable cells (assessed by Trypan blue dye exclusion) was determined in triplicate in a blinded fashion using a counting chamber under a magnification of ×200. The compound concentration that inhibits response at 72 hours by 50% (IC_{50}) corresponds to the fraction affected (F_a value) of 0.5. All

tested cells were exposed to nine different concentrations of PHA-739358 or to six concentrations of sorafenib. Immunostaining for cytokeratin 18 (1:50) followed the same protocol after treating cells with 50 nM PHA-739358 or DMSO for 48 hours, respectively.

Analysis of DNA Content, H3 Phosphorylation, and Apoptosis by Flow Cytometry

Analysis of DNA content and H3 phosphorylation was performed as previously described [9] with the following changes: Huh-7 and HepG2 cells were plated in their respective medium and exposed to PHA-739358 in increasing concentrations from 5 nM to 5 µM for 48 hours in all experiments. For analysis of apoptosis, cells were treated under the same conditions. After incubation with the drugs, cells were washed with PBS, fixed and permeabilized with FIX&PERM solutions (Invitrogen), respectively stained with anti–active caspase-3 phycoerythrin-conjugated specific antibody (BD Biosciences, San Jose, CA), and analyzed with flow cytometry.

Western Blot

Huh-7 and HepG2 cells were incubated with 50 or 500 nM PHA-739358 in the presence or absence of fetal calf serum for 6 and 24 hours, respectively. Total proteins were extracted from cells and untreated controls, and protein concentration was determined as described [15]. Proteins (30 µg) were resolved by sodium dodecyl sulfate/polyacryl gel electrophoresis (12% gel) and electrotransferred onto nitrocellulose membranes (pore size, 0.45 µm). Immunodetection was carried out using monoclonal and polyclonal antibodies [15] followed by peroxidase-conjugated secondary antibodies. Detection was performed using an enhanced chemiluminescence kit (Super Signal West Dura Extended Duration Substrate; Thermo Scientific, Rockford, MA).

Analysis of Stathmin Phosphorylation Status by Two-dimensional Gel Electrophoresis

Huh-7 and HepG2 cells were treated with up to 500 nM PHA-739358 for 48 hours or DMSO as control. Cells were lysed in sample buffer (9 M urea, 4% CHAPS, 0.5% Resolyte [Merck, Darmstadt, Germany], 10 µg/ml bromophenol blue). One hundred micrograms of total protein was loaded on an immobilized pH gradient (IPG) strip (pH 4-7, 7 cm; GE Healthcare, Solingen, Germany) by in-gel rehydration. After isoelectric focusing (Protean IEF Cell; Bio-Rad, Munich, Germany), immobilized pH gradient strips were equilibrated for 2 × 15 minutes in 6 M urea, 4% sodium dodecyl sulfate, 50 mM Tris-HCl pH 8.8 containing 1% 1,4-dithiothreitol or 4.8% iodoacetamide, respectively. Strips were placed on 15% sodium dodecyl sulfate/polyacryl gel electrophoresis gels and overlaid with 0.6% agarose. After transfer onto a polyvinylidene fluoride membrane (pore size, 0.45 µm; Millipore, Schwalbach, Germany), gels were stained with colloidal Coomassie to ensure equal protein loading. The membrane was incubated with antistathmin antibody (1:1000) overnight at 4°C followed by antirabbit HRP secondary antibody (Cell Signaling Technology). Detection was performed using Pierce ECL Western Blotting Substrate (Thermo Scientific).

Animals

The Animal Core of the Hamburg University Medical Center provided 6- to 10-week-old nonobese diabetic/severe combined immunodeficiency (NOD/SCID) mice. The animals were housed and treated under sterile conditions under a 12-hour light/12-hour dark schedule and were fed autoclaved chow and water *ad libitum*. All animal experiments were approved by the local authorities in accordance with the National Institutes of Health's Guide for Care and Use of Laboratory animals.

Tumor Xenografts

Tumors resulting after subcutaneous (SC) injection of Huh-7 or HepG2 cells in donor animals were aseptically dissected and mechanically minced. Pieces of tumor tissue, approximately 5 mm^3, were transplanted SC into the experimental animals by a trocar needle. Treatment was initiated when tumor volumes reached median sizes of 53 to 245 mm^3, and mice were assigned to treatment or control groups to obtain the closest possible mean tumor volume and SD. Body weight and tumor volume (length × width × height × 0.5236) were measured every 4 days using a caliper. If animals developed weight loss of more than 15% or tumor growth led to ulceration or disability of animals, mice were withdrawn from the experiments. At the end of each experiment, mice were killed under animal welfare guidelines, and necropsy was performed. Tumors were excised, weighed, snap frozen, and stored at –80°C.

Experimental Protocol

Experimental setting 1 (monotherapy). Mice bearing Huh-7 or HepG2 tumors were divided into a treatment group receiving PHA-739358 intraperitoneally at a dosage of 2 × 15 mg/kg per day or a control group receiving the same volume of vehicle solution (5% dextrose).

Experimental setting 2 (combination therapy). Mice bearing Huh-7 tumors were divided into four groups: group 1, control, vehicle solutions (12.5% Cremophor EL/12.5% ethanol in water by oral gavage plus 5% dextrose intraperitoneally); group 2, sorafenib by oral gavage at a dosage of 1 × 10 mg/kg per day; group 3, PHA-739358 at a reduced dosage of 1 × 15 mg/kg per day; and group 4, combination of sorafenib with PHA-739358 at the dosages used in groups 2 and 3, respectively.

Experimental setting 3 (sequential therapy). The same experimental design as in experimental setting 2 was used. However, after 8 days of treatment with sorafenib, therapy was stopped, and sequential treatment with PHA-739358 at the standard dosage (2 × 15 mg/kg per day) was initiated. Two independent experiments were performed.

Immunohistochemistry of Xenograft Tumors

Five-micrometer cryosections were fixed in acetone for 5 minutes at 4°C, washed twice for 5 minutes each in Tris-buffered saline containing 0.1% Tween-20, and blocked in H$_2$O$_2$ and bovine serum albumin. Primary antibodies (aurora-A and -B as previously mentioned, phospho-H3S10, 1:100) were applied for 1 hour at RT. Tissue sections were washed four times in PBS for 5 minutes and incubated with secondary antibodies (Alexa Fluor 488 goat IgG, 1:500; Cy3-AffiniPure goat IgG, 1:500; Dako Real Envision) for 30 minutes. Sections were washed four times for 5 minutes in PBS, counterstained with H&E or Hoechst-33258 (Molecular Probes, Eugene, OR) and examined under light microscopy or epifluorescence, respectively.

Statistical Methods

Significance of differences was analyzed by χ^2 tests, Fisher exact test, or 2-tailed Student's *t* tests. $P < .05$ was considered significant.

Results

Aurora Kinase Expression in Primary Human HCCs and HCC Cell Lines

The TMA contained a total of 93 primary human HCC tumor spots (Figure 1*A*), 89 of which were interpretable for both aurora kinases and Ki-67 expression. Aurora-A was highly expressed in virtually all HCCs with a pronounced staining in the cytoplasm in most histospots, although nuclear staining was also observed (Figure 1*B*). Weak cytoplasmic but no nuclear expression of aurora-A was found in each of the 10 nontumorous cirrhotic control liver samples. Aurora-B expression was strictly nuclear (Figure 1*C*). A total of 21 HCCs (23.6%) were positive for aurora-B, whereas cirrhotic livers did not reveal aurora-B expression. The proliferation index indicated by Ki-67 expression served as a biomarker for tumor aggressiveness (Figure 1*D*). Aurora-B was expressed in 3 (6.0%) of 50 low proliferating tumors (2x +, 1x ++), in 12 (36.3%) of 33 moderately proliferating tumors (8x +, 4x ++), and in 6 (100%) of 6 highly proliferating tumors (2x +, 4x ++; $P < .001$; χ^2 test 2xk table for all proliferation index groups; $P < .001$, moderate *vs* low; $P < .001$, high *vs* low; $P = .005$, high *vs* moderate; Fisher exact test).

The human HCC–derived cell lines Huh-7 and HepG2 were tested positive for aurora-A and aurora-B (Figure 2). Aurora-A, which localizes to the centrosome during interphase until the early mitotic phase of the cell cycle, was visible as multiple intranuclear spots, but cytoplasmic staining was also observed (Figure 2*A*). In later stages of mitosis, aurora-A was located at the spindle poles (Figure 2*A*, *arrows*).
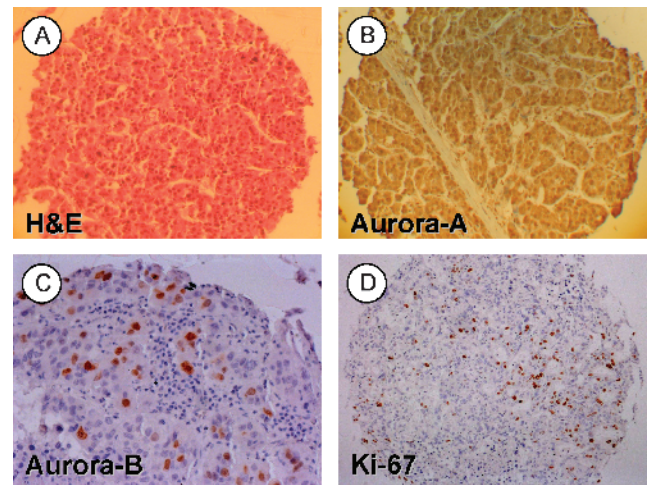

Figure 1. Human HCC TMA. Representative samples of (A) an H&E–stained HCC tissue spot (original magnification, ×100), (B) a HCC spot showing marked nuclear and cytoplasmic aurora-A protein localization (original magnification, ×100), (C) a tumor spot with strong (++) expression of aurora-B (original magnification, ×200), and (D) a respective tumor spot stained for the proliferation marker Ki-67 (MIB-1; original magnification, ×100). Panels B to D were counterstained with hematoxylin.
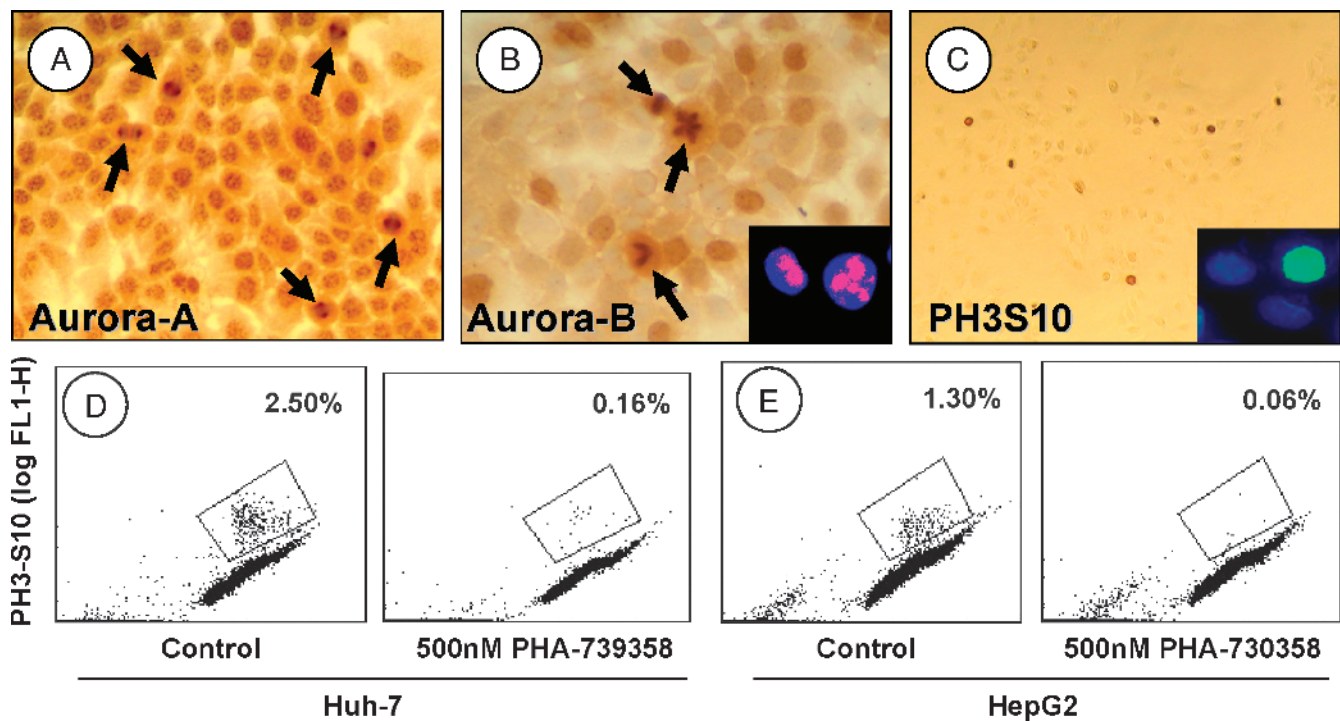

Figure 2. Aurora kinase expression in human HCC cells. (A) Huh-7 cells expressing aurora-A, which localizes to the centromeres or to the spindle pole (arrows; see text). (B) Aurora-B expression until the metaphase is seen as diffuse brown nuclear staining in Huh-7 (large panel) and HepG2 (insert, left cell) cells or in the spindle midzone during late mitosis (Huh-7, arrows; HepG2, insert, right cell). (C) Nuclear staining for phospho-H3S10 in Huh-7 and HepG2 (insert) cells quantified by flow cytometric analysis (D and E): Huh-7 (D) and HepG2 (E) cells, double stained with propidium iodide (DNA content) and anti–phospho-H3S10. Left panels show controls; right panels show the respective cells treated with 500 nM PHA-739358. The gates indicate phospho-H3S10–positive cells. Original magnifications: ×200 (A), ×400 (B), ×100 (C), ×600 (inserts).

Aurora-B was localized to the centromeres until metaphase and, therefore, was seen mainly as diffuse nuclear staining (Figure 2B). In anaphase and telophase, when aurora-B localizes to the spindle midzone or midbody, it became clearly visible (Figure 2B, arrows). Aurora-A and -B expression was confirmed by Western blot of nuclear lysates (not shown).

Downstream target histone H3, which is phosphorylated at Ser10 (phospho-H3S10) by aurora-B during mitosis [16], was expressed in both HCC cell lines (Figure 2C). Quantitative analysis of phospho-H3S10 revealed a cell fraction of 2.5% in Huh-7 and 1.3% in HepG2 cells by flow cytometry, indicating aurora-B activity in both human HCC cell lines (Figure 2, D and E).

Inhibition of Tumor Cell Proliferation by PHA-739358

The effect of different concentrations of aurora kinase inhibition by PHA-739358 on HCC cell proliferation was determined by Trypan blue exclusion assay. At concentrations starting from 50 nM, PHA-739358 led to an almost complete stop of proliferation in both Huh-7 and HepG2 cells ($P < .001$, Huh-7; $P = .003$, HepG2 at 96 hours; Figure 3A). Analysis of the dose-response relationship revealed an approximate IC_{50} at 72 hours of 15 nM for Huh-7 and 20 nM for HepG2 cells. PHA-739358 treatment changed the morphology of tumor cells, resulting in large nuclei and an increased nucleus-to-cytoplasm ratio compared with untreated controls, suggesting that cells have undergone endoreduplication (Figure 3B). After withdrawal of PHA-739358 from cells treated with 500 nM for 48 hours, neither Huh-7 nor HepG2 cells restarted to grow, indicating a persistent treatment effect.

PHA-739358 Induces Endoreduplication of Tumor Cells and Inhibits Phosphorylation of H3S10

To further elucidate the potential mechanisms of action of PHA-739358, we next performed cell cycle analysis by flow cytometry (Figure 4A). Significant inhibition of cell proliferation started from 50 nM, leading to endoreduplication of cells with a substantial increase of the DNA content (4N and >4N fractions), whereas higher concentrations exceeding 500 nM caused a complete G_2/M–phase arrest (Figure 4A).

Inhibition of H3S10 phosphorylation was observed in both HCC cell lines secondary to treatment with PHA-739358 (Figures 2, D and E, and 4B). However, although 50 nM effectively suppressed cell
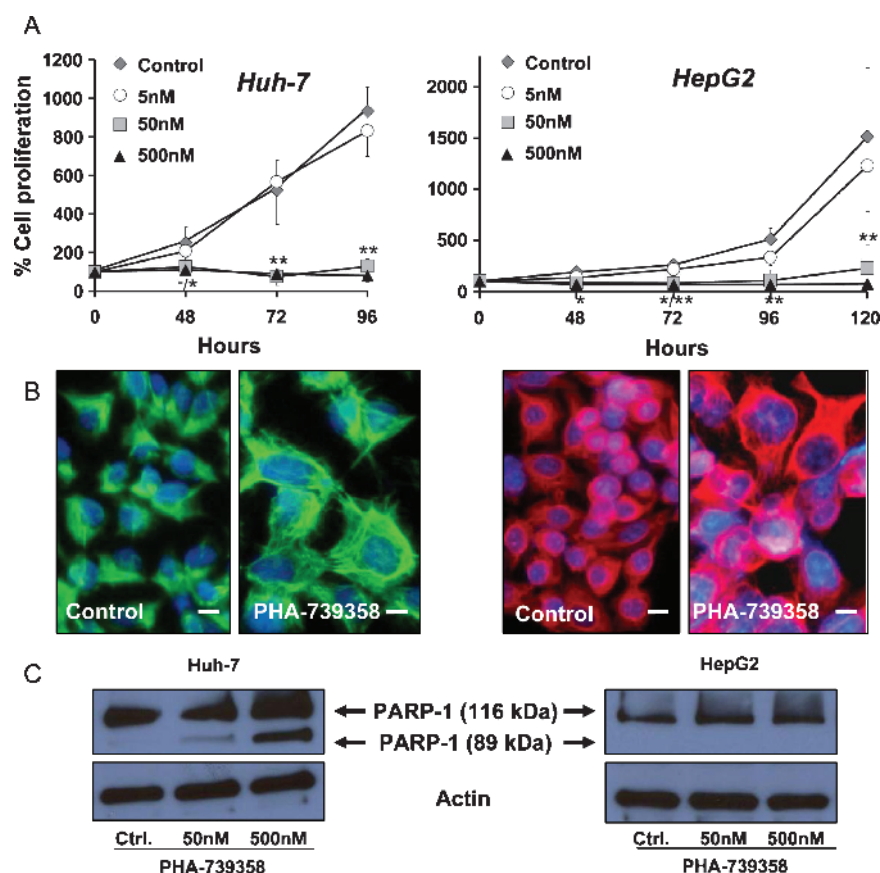

Figure 3. Antiproliferative effects of PHA-739358 treatment *in vitro*. Left panels, Huh-7; right panels, HepG2. (A) Antiproliferative effect of PHA-739358 in rapidly proliferating Huh-7 cells (analyzed after 96 hours) and moderately proliferating HepG2 cells (for up to 120 hours). Significant antiproliferative effects of PHA-739358 at 50 and 500 nM compared with DMSO controls. *$P < .05$; **$P < .01$ of 50 nM/ 500 nM PHA-739358 compared with controls. (B) Immunohistochemistry for cytokeratin 18 as a cytoplasmic marker of HCC cells treated with DMSO control or 50 nM PHA-739358. Treatment with the compound for 48 hours resulted in large nuclei in Huh-7 (green) and HepG2 cells (red) indicating endoreduplication. Original magnification, ×400; scale bars, 10 μm; counterstained with Hoechst-33258. (C) Effects of PHA-739358 treatment for 24 hours on PARP-1 cleavage as an indicator of caspase mediated apoptosis. The 116-kDa band indicates full-length PARP-1; the 89-kDa band represents the large fragment of PARP-1, which results only in PHA-739358–treated Huh-7 but not in HepG2 cells.
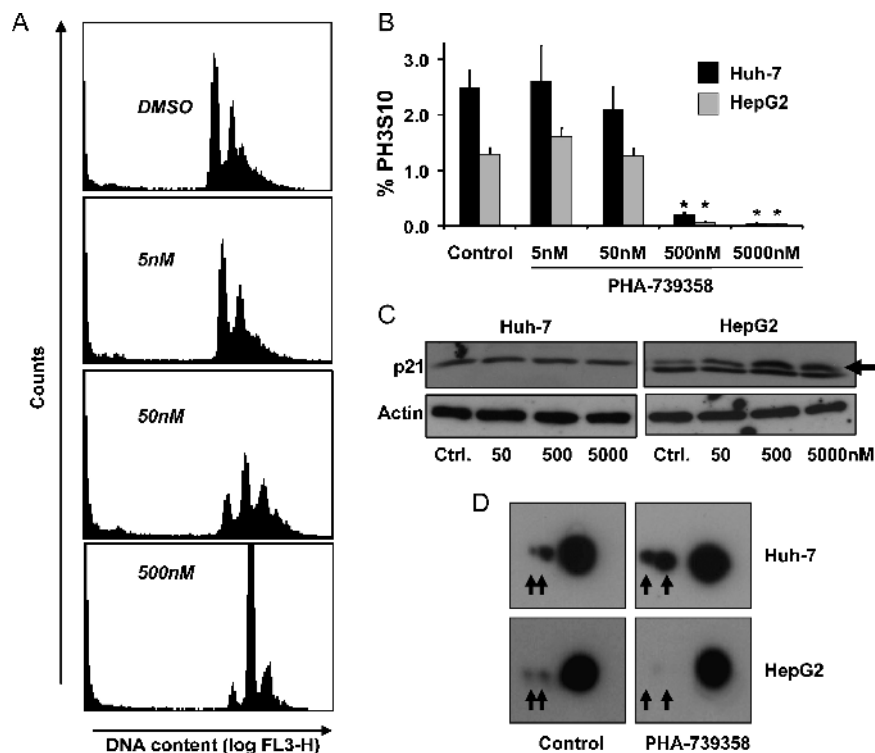
Figure 4. Mechanisms of PHA-739358 treatment. (A) Cell cycle profile of Huh-7 cells mediated by the compound after 48 hours at the indicated concentrations. DNA content was assessed by flow cytometry. (B) Percentage of phospho-H3S10–positive Huh-7 and HepG2 cells after treatment with DMSO or PHA-739358 at the indicated concentrations for 2 hours. Significant inhibition of phospho-H3S10 starts from PHA-739358 concentrations of 500 nM (*P < .01). (C) Western blot of lysates from HCC cells treated for 48 hours with the indicated concentrations of PHA-739358. p21 (upper band; arrow) was only induced in p53 wild-type HepG2 cells (the lower band in HepG2 lysates is unspecific). (D) Two-dimensional gel electrophoresis and stathmin staining of protein lysates from HCC cells treated with 500 nM PHA-739358 for 2 hours. The small dots (arrows) indicate the two stathmin phosphorylation sites and show a loss of phosphorylation in HepG2 cells.

proliferation, a significant inhibition of H3S10 phosphorylation was only observed for concentrations exceeding 10-fold this dose level (phospho-H3S10 cell fraction at 500 nM: Huh-7: 0.16% vs 2.50% in controls, P < 01; HepG2: 0.06% vs 1.30%, P < .01; n = 3 each; approximate phospho-H3S10 IC$_{50}$ in both HCC cell lines, 100 nM).

Induction of apoptosis in PHA-739358–treated HCC cells was assessed by Western blot for fragmentation of poly(ADP-ribose) polymerase 1 (PARP-1), a main caspase cleavage target. p53 mutated Huh-7 cells treated with increasing concentrations of PHA-739358 for 24 hours indicated distinct PARP-1 fragmentation (Figure 3C), whereas the fraction of caspase-3–stained cells as assessed by flow cytometry was only moderately increased (3.2 ± 0.4%, 4.4 ± 0.3%, and 5.7 ± 0.7% for 50 nM, 500 nM, and 5 μM, respectively, compared with 1.5 ± 0.1% in DMSO controls, P < .05). In contrast, in p53 wild-type HepG2 cells, PHA-739358 did not lead to an increase of PARP-1 cleavage (Figure 3C) or caspase-3–stained cell fractions.

Effects of PHA-739358 on Signaling Pathways, Cell Cycle Regulators, and Stathmin Phosphorylation

To investigate a possible role of PHA-739358 on the mitogenic signaling cascade as a mechanism of action, Huh-7 and HepG2 cells were treated with various concentrations of the compound for up to 48 hours, and phosphorylation of downstream proteins was analyzed by Western blot. Interestingly, phosphorylation of extracellular signal-regulated kinases, protein kinase B, and c-Jun N-terminal kinases remained unchanged (data not shown), indicating that inhibition of cell

proliferation by PHA-739358 was not based on altered activation of these mitogenic pathways.

To evaluate the alternative mechanisms for the observed effects, we analyzed the effect of PHA-739358 on cell cycle–associated proteins. Expressions of the cyclin-dependent kinase p27, a cell cycle inhibitor, and p16, which plays a crucial role in the process of cell cycle progression at the G$_1$/S checkpoint, were not altered (data not shown), whereas p21, a p53-controlled regulator of cell cycle progression, was induced by PHA-739358 treatment in p53 wild-type HepG2 cells, although it remained unchanged in p53 mutated Huh-7 cells (Figure 4C).

G$_2$/M–phase arrest results from perturbations of tubulin polymerization as part of the cellular spindle apparatus, which is regulated by the microtubule destabilizing protein stathmin/Op18 [17]. Because stathmin is overexpressed in human hepatocarcinogenesis and phosphorylated by aurora-B [18,19], we determined the effect of PHA-739358 treatment on stathmin phosphorylation in HCC cells. To facilitate microtubule formation during mitosis, stathmin needs to be inactivated by phosphorylation. After completion of mitosis, stathmin is dephosphorylated, the spindles disintegrate, and cytokinesis can be accomplished [20]. Two-dimensional gel electrophoresis did not show inhibition of phosphorylation by PHA-739358 in Huh-7 cells, whereas in HepG2 cells, which exhibited a lower baseline phosphorylation status compared with Huh-7 cells, PHA-739358 treatment for 48 hours led to a loss of stathmin phosphorylation compared with DMSO-treated controls (Figure 4D).

Immunohistochemical Characterization of Tumor Xenografts

Both cell lines were injected into the flanks of immunodeficient NOD/SCID mice. The histochemical properties of resulting tumors resembled those of the primary cell lines. Aurora-A was expressed in all nuclei of transplanted cells, whereas the surrounding recipient tissue was negative for aurora-A expression (Figure 5A). Xenografts showed aurora-B expression in 16.5 ± 5.8% and 10.6 ± 2.9% of the nuclei in Huh-7 and HepG2 tumors, respectively (Figure 5B). The phosphorylation status of H3S10 was slightly increased in xenografts compared with primary cells (4.3 ± 1.5%; Huh-7, 2.6 ± 1.3%; HepG2; n = 8 tumors each; Figure 5C).

Inhibition of Tumor Growth in Experimental Models of HCC

In experimental setting 1, treatment with PHA-739358 at a dosage of 2 × 15 mg/kg per day significantly decreased tumor growth of both, rapidly proliferating Huh-7 tumors and moderately growing HepG2 xenografts (Figure 5D). Huh-7 tumor growth was significantly inhibited from day 3 ($P < .05$) until the end of the experiment ($P < .01$). The mean absolute tumor volume was reduced by 80.4%, the mean percent tumor growth was reduced by 84.4%, and the mean tumor weight on necropsy was reduced by 71.8%, respectively, compared with vehicle-treated controls (Figure 5D; Table 1). Antiproliferative efficacy was even more pronounced in HepG2 tumors at the same dosage level (statistical details in Table 1).

In experimental setting 2, PHA-739358 in combination with sorafenib was evaluated. In a preparatory experiment, antiproliferative efficacy of sorafenib was confirmed in Huh-7 cells *in vitro* and *in vivo* at a dose of 30 mg/kg [21] (data not shown). Monotherapy

with both, sorafenib tosylate at a dosage of 10 mg/kg per day or with a reduced dosage of PHA-739358 investigated for combination therapy (15 mg/kg given once daily), did not lead to growth arrest but to a significant deceleration of Huh-7 tumor proliferation (Figure 6A; Table 1). Remarkably, the combination of PHA-739358 with sorafenib tosylate virtually stopped growth of Huh-7 tumors completely until treatment was terminated at day 20 ($P < .001$ *vs* PHA-739358 or *vs* sorafenib alone, respectively; Table 1). After cessation of therapy, tumors began to regrow, however, at a very slow rate (Figure 6A, day 24).

In experimental setting 3, one group of Huh-7 tumor-bearing mice received the aforementioned combined treatment with PHA-739358 and sorafenib. The significantly superior effect described in experimental setting 2 compared with the respective monotherapies was confirmed (Figure 6B). To determine the impact of aurora kinase inhibition on HCCs, which still proliferate *in vivo* under sorafenib monotherapy, sorafenib treatment was replaced on day 8 by the dosage of PHA-739358 shown to be effective in experimental setting 1 (2 × 15 mg/kg per day). Remarkably, this PHA-739358 "salvage" therapy not only stopped tumor proliferation entirely but also virtually shrank tumor volumes by up to 81% in all nine sequentially treated xenografts (40.1 ± 25.7%; Figure 6B). Furthermore, these tumors were found to be macroscopically and microscopically entirely necrotic (not shown).

Discussion

Recently, the SHARP trial demonstrated for the first time that targeted therapy can extend overall survival in patients with HCC [4], and as a consequence, sorafenib is currently considered the reference criterion standard of systemic therapy [3]. However, nonresponse,
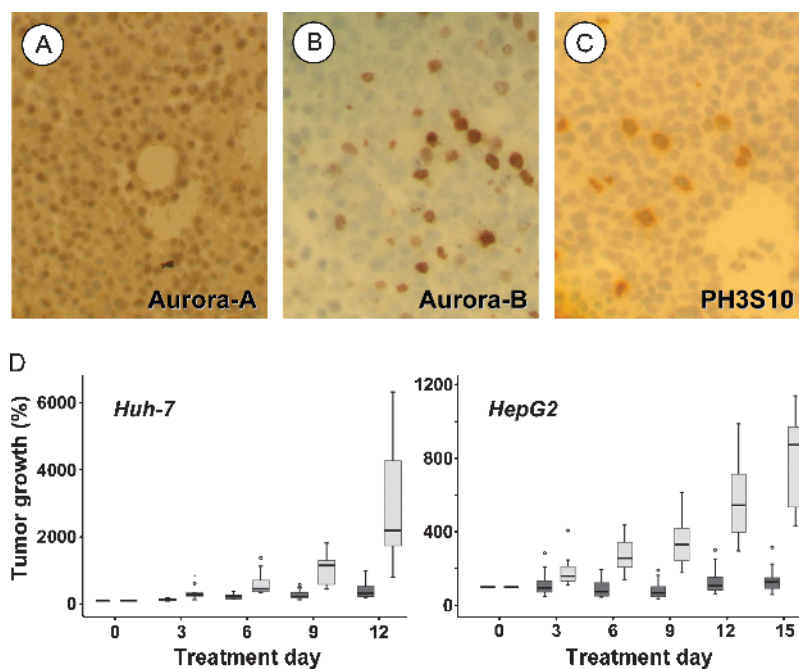

Figure 5. HCC xenograft model. (A–D) Immunohistochemistry of Huh-7 tumors grown after SC injection into NOD/SCID mice, with specific antibodies for aurora-A (A), aurora-B (B), and phospho-H3S10 (C). Comparable results were found in HepG2 tumors (see text). (D) PHA-739358 effectively inhibits growth of Huh-7 (D; n = 11 *vs* n = 10 controls) and HepG2 (n = 12 *vs* n = 12 controls) tumors *in vivo*. Box plots indicating median, upper and lower quartiles, as well as lowest and highest observations. Small circles indicate mild outliers; no extreme outliers were observed. PHA-739358 at a dosage of 15 mg/kg twice per day (dark gray bars) was well tolerated and significantly suppressed tumor growth compared with vehicle-treated controls (light gray bars; see text). Different end points for the two cell lines were due to the differential growth rate of Huh-7 or HepG2 tumors, respectively.

Table 1. Effects of Therapy with PHA-739358 on the Growth of Human HCCs Xenografted in NOD/SCID Mice.

Experiment	Initial Volume (mm³)	Final Volume (mm³)	Final (% Growth)	Tumor Weight (mg)
Setting 1				
Control (Huh-7)	60.7 ± 43.2	1182.9 ± 687.6	2175 ± 1839	1298 ± 712
PHA-739358 (Huh-7)	52.5 ± 32.4	232.1 ± 211.2†	340 ± 307†	366 ± 333*
Control (HepG2)	111.6 ± 62.7	908.7 ± 621.1	873 ± 250	1484 ± 1046
PHA-739358 (HepG2)	106.0 ± 80.7	106.4 ± 39.6‡	137 ± 72‡	119 ± 34‡
Setting 2				
Control	291.3 ± 285.7	Treatment stopped on day 12 owing to high tumor volume		
PHA-739358 1 × 15 mg/kg	245.6 ± 239.0	680.7 ± 421.9¶	391 ± 122¶	1183 ± 1021$^\#$
Sorafenib 1 × 10 mg/kg	212.1 ± 179.9	704.4 ± 644.2¶	454 ± 216¶	1326 ± 1078$^\#$
Combination	243.0 ± 139.7	256.4 ± 256.9¶	97 ± 64¶,§	281 ± 612$^\#$

Setting 1: Monotherapy of PHA-739358 at the standard dosage of 2 × 15 mg/kg per day.
Setting 2: Combination therapy of PHA-739358 at a reduced dosage with sorafenib.
Values were presented as mean ± SD.
*$P < .05$ *versus* controls.
$^†P < .01$ *versus* controls.
$^‡P < .001$ *versus* controls.
$^§P < .01$ *versus* PHA-739358 and *versus* sorafenib, respectively.
¶Final volumes in Setting 2 were obtained on day 20 when treatment was stopped.
$^\#$Tumor weights were obtained after killing on day 24.
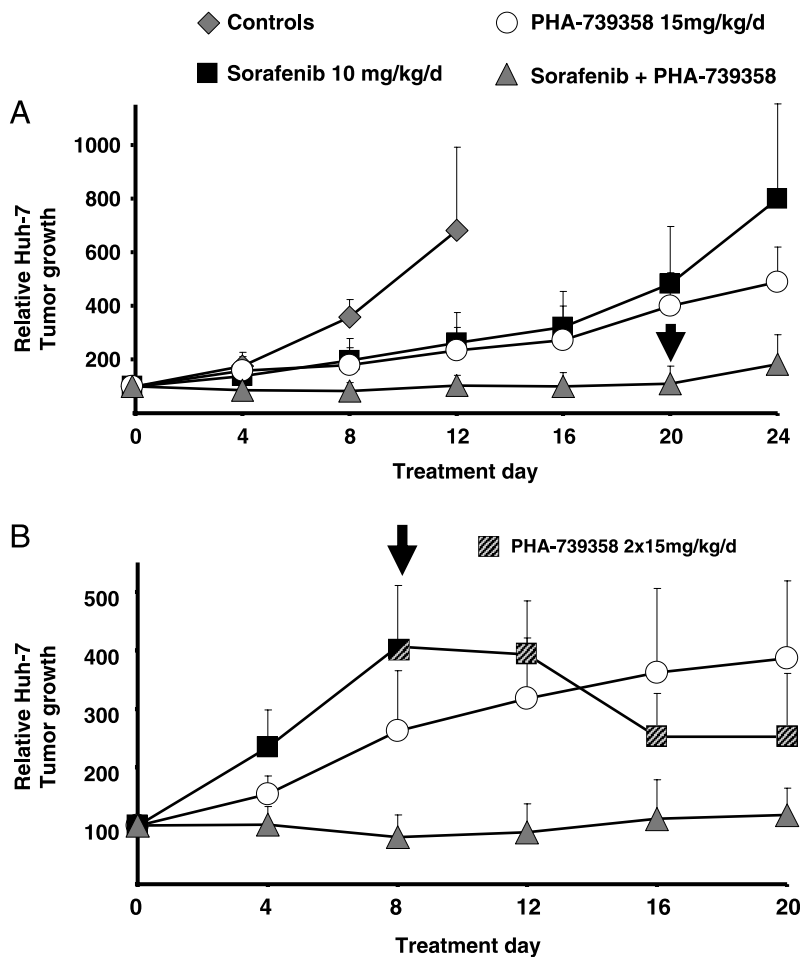

Figure 6. Combination therapy with PHA-739358 and sorafenib. (A) Vehicle-treated control tumors grew rapidly, and mice were killed on day 12 after initiation of treatment because of disabling tumor burden in some animals ($n = 7$). PHA-739358 at a reduced dosage of 15 mg/kg per day ($n = 8$) and sorafenib at a dosage of 10 mg/kg per day ($n = 7$) decelerated tumor growth. Combination therapy with PHA-739358 and sorafenib ($n = 9$) led to complete growth arrest. After cessation of combination therapy (arrow), some tumors began to grow at a very slow rate (see Table 1 and text for statistical data). (B) The same experimental setting as in panel A was used, and the growth arrest of tumors under combination therapy was confirmed ($n = 9$ in all treatment groups). However, sorafenib monotherapy was stopped on day 8 when tumors quadrupled their size (arrow). Replacement of therapy with PHA-739358 at the standard monotherapy dosage of 15 mg/kg twice per day from day 8 (striped boxes) until the end of the experiment induced shrinkage of tumors (see text). All values are presented as mean +SD.

early resistance, or intolerance to sorafenib is a significant clinical problem emphasizing the demand for additional and/or alternative treatment strategies.

Overexpression of aurora kinases has been demonstrated in a variety of human malignancies [7]. To assess the impact of aurora kinases as a potential molecular target in HCC, we screened a TMA consisting of a large series of human HCC tumor specimen for expression of aurora kinases. Aurora-A overexpression, an early event in carcinogenesis, was detected in all HCCs, whereas Jeng et al. [10] found aurora-A gene expression in only 61% of 224 HCCs studied. Whether the nonquantitative assessment of messenger RNA correlates with protein expression of aurora-A needs to be discussed because Western blot or immunohistochemistry had not been performed in this study. Interestingly, positivity for aurora-A messenger RNA was associated with higher grading, advanced tumor stage, and poor outcome [10].

Recent studies indicate that the inhibition of aurora-B might represent a highly promising anticancer strategy [22,23]. Here, we demonstrate that aurora-B expression is significantly associated with a high proliferation index, which has been linked to adverse clinical outcome in HCCs [24,25]. In line with our findings in HCC, aurora-B expression was also found to correlate with tumor cell proliferation in other malignancies resulting in higher tumor grading and a poor prognosis [7,26,27]. Tanaka et al. [11] recently identified aurora-B gene expression in curatively resected HCCs as the most significant predictor for aggressive tumor recurrence or genetic instability. Furthermore, validation studies even demonstrated an association of aurora-B expression with significantly impaired survival. Notably, amplification of chromosomes 17q and 20q, where aurora-A and -B genes are localized, are among the most common cytogenetic aberrations in human HCC and have been linked to dedifferentiation [28,29].

Recently, Lin et al. [12] reported the first promising results using high doses of AKI VE-465, an analog of VX-680. To our knowledge, no clinical trial activity is currently being pursued with these compounds. On the contrary, we evaluated here the *in vitro* and *in vivo* efficacy of AKI PHA-739358, which has now entered phase 1/2 clinical trials for relapsing chronic myeloid leukemia and metastatic prostate cancer [30,31]. *In vitro* antiproliferative efficacy of PHA-739358 was demonstrated at nanomolar concentrations in both p53 wild-type HepG2 cells and p53 mutated Huh-7 cells. Discrimination of the p53 status is crucial because p53 is frequently mutated in human HCC [32,33], and functional interaction between p53 and aurora kinases has been described [34–36]. In fact, selective inhibition of aurora-A provided a growth advantage in some tumor cells that experienced loss of p53 [36].

PHA-739358 significantly inhibited phosphorylation of the aurora-B target histone H3 at concentrations exceeding 500 nM resulting in a complete G_2/M–phase arrest. In contrast, lower concentrations led to inhibition of cell division and endoreduplication without measurably affecting histone H3 phosphorylation. This effect has been attributed to aurora-A inhibition with the aurora-A–regulated spindle apparatus being the primary target. Accordingly, our analyses showed a DNA content of 4N or more in massively enlarged nuclei of tumor cells. Indeed, quantitative kinase inhibition assay previously demonstrated variable sensitivity of aurora kinases for PHA-739358 (IC_{50} value of 13 nM for aurora-A and 79 nM for aurora-B, respectively) [8]. In a current phase 2 clinical trial, PHA-739358 serum levels of up to 5000 nM were achievable and well tolerated in humans [37]. Thus, considering the IC_{50} values outlined here, the therapeutic range of

the compound will most likely be sufficient to exert a pan-aurora activity *in vivo*. Notably, high concentrations in the micromolar range were required for *in vitro* effectiveness of the AKI used by Lin et al., which exhibits 26× stronger inhibition of aurora A compared with aurora B. These findings might explain the more potent *in vitro* activity of PHA-739358 in the cellular system.

The effect of PHA-739358 is not limited to aurora kinases but also extends to other cellular kinases, such as Ret, fibroblast growth factor receptors, Abl, or tyrosine kinase A [8]. To further elucidate additional mechanisms of action in HCC, we analyzed downstream targets of mitogenic signaling pathways, which, like aurora kinases, are phosphorylated at serine or threonine sites and are relevant to HCC cells [38,39]. However, neither extracellular signal-regulated kinases (downstream target of Ras/Raf signaling, fibroblast growth factor receptor, src), nor c-Jun N-terminal kinases (several growth factors and cell surface receptors, src) or protein kinase B (phosphatidylinositol-3 kinase, fibroblast growth factor receptor), which has been shown to be activated by aurora-A [40], were significantly influenced. Interestingly, PHA-739358 induced apoptosis only in Huh-7 cells but not in HepG2 cells in the concentrations used here. Similarly, Lin et al. [12] reported apoptosis in HepG2 cells only at very high concentrations of 10 mM. This may be attributed to the variable p53 status of the two cell lines [41,42]. Mechanistically, we found that p21, a transcriptional target of p53 involved in experimental and human hepatocarcinogenesis [43,44], was distinctly induced by PHA-739358 treatment in p53 wild-type HepG2 cells but not in p53 mutated Huh-7 cells. Because p53 is destabilized by aurora-A–dependent phosphorylation, this may explain the differential response in these cell lines [35,45]. Gizatullin et al. [46] demonstrated that tumor cells lacking an intact p53-p21 pathway were more likely to undergo apoptosis and endoreduplication in response to aurora kinase inhibition, whereas the integrity of this pathway in some cell lines resulted in less endoreduplication. This may also explain why PHA-739358 inhibited stathmin phosphorylation only in p53 wild-type HepG2 cells but not in Huh-7 cells, where stathmin is upregulated as a result of p53 mutation [19]. Stathmin is phosphorylated by aurora-B [18], overexpressed in human hepatocarcinogenesis [19], and is of prognostic relevance for patients with HCC [47]. Thus, inhibition of stathmin phosphorylation by PHA-739358 may represent an additional mechanism of aurora kinase targeting in p53 wild-type HCC cells [20].

Efficacy and toxicity of PHA-739358 were then evaluated in a SC HCC xenograft model showing high antiproliferative activity at well-tolerated doses. Inhibition of tumor growth in rapidly proliferating Huh-7 tumors was highly significant although tumors continued to grow at a very slow rate, which is comparable to the results attained by Lin et al. [12]. To further substantiate the *in vivo* effectiveness of aurora kinase inhibition in HCC, we also analyzed the effectiveness in a second HCC cell line *in vivo*, that is, the more slowly proliferating HepG2 tumors. Although complete growth inhibition was achieved in these tumors, no significant tumor regression was observed. These findings are in line with the moderate or missing apoptosis in Huh-7 or HepG2 cells as well as with the results from Lin et al., who observed complete PARP cleavage *in vitro* but only very minor apoptosis *in vivo* (<3% to 4%, depending on the dosage) [12]. In our experiments, the combination of PHA-739358 with sorafenib showed a synergistic effect. Notably, sorafenib at the given dose of 10 mg/kg only led to a modest slowdown of tumor growth in mice [21], a dose range comparable to the dosage applied in humans [4]. However, the combination of sorafenib and PHA-739358 caused a virtual growth arrest

of HCC tumors. Furthermore, standard monotherapy dose of PHA-739358 alone was capable of shrinking tumors even after treatment failure under sorafenib. The *in vivo* mechanisms of sorafenib are well studied, namely, vascular endothelial growth factor/platelet-derived growth factor–mediated tumor angiogenesis and Raf kinase signaling. The simultaneous targeting of cell cycle–associated events by PHA-739358 may complement these mechanisms. Comparably, Villanueva et al. [48] reported synergistic effects of proapoptotic and antiproliferative mechanisms in HCC xenografts using combined inhibition of the mammalian target of rapamycin and epidermal growth factor receptor.

In conclusion, targeted inhibition of aurora kinases by PHA-739358, alone or in combination, may offer a promising new approach for the treatment of patients with advanced stage HCC. In addition, the high efficacy of the AKI secondary to sorafenib failure raises hope for an effective second-line therapy and provides rationales for future clinical trials using PHA-739358 in this tumor entity.

Acknowledgments

References

[1] El-Serag HB and Rudolph KL (2007). Hepatocellular carcinoma: epidemiology and molecular carcinogenesis. *Gastroenterology* **132**, 2557–2576.

[2] Leong TY and Leong AS (2005). Epidemiology and carcinogenesis of hepatocellular carcinoma. *HPB (Oxford)* **7**, 5–15.

[3] Llovet JM and Bruix J (2008). Molecular targeted therapies in hepatocellular carcinoma. *Hepatology* **48**, 1312–1327.

[4] Llovet JM, Ricci S, Mazzaferro V, Hilgard P, Gane E, Blanc JF, de Oliveira AC, Santoro A, Raoul JL, Forner A, et al. (2008). Sorafenib in advanced hepatocellular carcinoma. *N Engl J Med* **359**, 378–390.

[5] Zhu AX (2008). Development of sorafenib and other molecularly targeted agents in hepatocellular carcinoma. *Cancer* **112**, 250–259.

[6] Keen N and Taylor S (2004). Aurora-kinase inhibitors as anticancer agents. *Nat Rev Cancer* **4**, 927–936.

[7] Gautschi O, Heighway J, Mack PC, Purnell PR, Lara PN Jr, and Gandara DR (2008). Aurora kinases as anticancer drug targets. *Clin Cancer Res* **14**, 1639–1648.

[8] Carpinelli P, Ceruti R, Giorgini ML, Cappella P, Gianellini L, Croci V, Degrassi A, Texido G, Rocchetti M, Vianello P, et al. (2007). PHA-739358, a potent inhibitor of Aurora kinases with a selective target inhibition profile relevant to cancer. *Mol Cancer Ther* **6**, 3158–3168.

[9] Gontarewicz A, Balabanov S, Keller G, Colombo R, Graziano A, Pesenti E, Benten D, Bokemeyer C, Fiedler W, Moll J, et al. (2008). Simultaneous targeting of Aurora kinases and Bcr-Abl kinase by the small molecule inhibitor PHA-739358 is effective against imatinib-resistant BCR-ABL mutations including T315I. *Blood* **111**, 4355–4364.

[10] Jeng YM, Peng SY, Lin CY, and Hsu HC (2004). Overexpression and amplification of Aurora-A in hepatocellular carcinoma. *Clin Cancer Res* **10**, 2065–2071.

[11] Tanaka S, Arii S, Yasen M, Mogushi K, Su NT, Zhao C, Imoto I, Eishi Y, Inazawa J, Miki Y, et al. (2008). Aurora kinase B is a predictive factor for the aggressive recurrence of hepatocellular carcinoma after curative hepatectomy. *Br J Surg* **95**, 611–619.

[12] Lin ZZ, Hsu HC, Hsu CH, Yeh PY, Huang CY, Huang YF, Chen TJ, Kuo SH, Hsu C, Hu FC, et al. (2009). The Aurora kinase inhibitor VE-465 has anticancer effects in pre-clinical studies of human hepatocellular carcinoma. *J Hepatol* **50**, 518–527.

[13] Carlomagno F, Anaganti S, Guida T, Salvatore G, Troncone G, Wilhelm SM, and Santoro M (2006). BAY 43-9006 inhibition of oncogenic RET mutants. *J Natl Cancer Inst* **98**, 326–334.

[14] Holst F, Stahl PR, Ruiz C, Hellwinkel O, Jehan Z, Wendland M, Lebeau A, Terracciano L, Al-Kuraya K, Janicke F, et al. (2007). Estrogen receptor α (*ESR1*) gene amplification is frequent in breast cancer. *Nat Genet* **39**, 655–660.

[15] Huber S, Schrader J, Fritz G, Presser K, Schmitt S, Waisman A, Luth S, Blessing M, Herkel J, and Schramm C (2008). P38 MAP kinase signaling is required for the conversion of CD4+CD25− T cells into iTreg. *PLoS ONE* **3**, e3302.

[16] Hirota T, Lipp JJ, Toh BH, and Peters JM (2005). Histone H3 serine 10 phosphorylation by Aurora B causes HP1 dissociation from heterochromatin. *Nature* **438**, 1176–1180.

[17] Redeker V, Lachkar S, Siavoshian S, Charbaut E, Rossier J, Sobel A, and Curmi PA (2000). Probing the native structure of stathmin and its interaction domains with tubulin. Combined use of limited proteolysis, size exclusion chromatography, and mass spectrometry. *J Biol Chem* **275**, 6841–6849.

[18] Gadea BB and Ruderman JV (2006). Aurora B is required for mitotic chromatin-induced phosphorylation of Op18/Stathmin. *Proc Natl Acad Sci USA* **103**, 4493–4498.

[19] Singer S, Ehemann V, Brauckhoff A, Keith M, Vreden S, Schirmacher P, and Breuhahn K (2007). Protumorigenic overexpression of stathmin/Op18 by gain-of-function mutation in p53 in human hepatocarcinogenesis. *Hepatology* **46**, 759–768.

[20] Rubin CI and Atweh GF (2004). The role of stathmin in the regulation of the cell cycle. *J Cell Biochem* **93**, 242–250.

[21] Liu L, Cao Y, Chen C, Zhang X, McNabola A, Wilkie D, Wilhelm S, Lynch M, and Carter C (2006). Sorafenib blocks the RAF/MEK/ERK pathway, inhibits tumor angiogenesis, and induces tumor cell apoptosis in hepatocellular carcinoma model PLC/PRF/5. *Cancer Res* **66**, 11851–11858.

[22] Girdler F, Gascoigne KE, Eyers PA, Hartmuth S, Crafter C, Foote KM, Keen NJ, and Taylor SS (2006). Validating Aurora B as an anti-cancer drug target. *J Cell Sci* **119**, 3664–3675.

[23] Yang H, Burke T, Dempsey J, Diaz B, Collins E, Toth J, Beckmann R, and Ye X (2005). Mitotic requirement for aurora A kinase is bypassed in the absence of aurora B kinase. *FEBS Lett* **579**, 3385–3391.

[24] Guzman G, Alagiozian-Angelova V, Layden-Almer JE, Layden TJ, Testa G, Benedetti E, Kajdacsy-Balla A, and Cotler SJ (2005). p53, Ki-67, and serum α feto-protein as predictors of hepatocellular carcinoma recurrence in liver transplant patients. *Mod Pathol* **18**, 1498–1503.

[25] Schmitt-Graff A, Ertelt V, Allgaier HP, Koelble K, Olschewski M, Nitschke R, Bochaton-Piallat ML, Gabbiani G, and Blum HE (2003). Cellular retinol-binding protein-1 in hepatocellular carcinoma correlates with β-catenin, Ki-67 index, and patient survival. *Hepatology* **38**, 470–480.

[26] Chieffi P, Cozzolino L, Kisslinger A, Libertini S, Staibano S, Mansueto G, De Rosa G, Villacci A, Vitale M, Linardopoulos S, et al. (2006). Aurora B expression directly correlates with prostate cancer malignancy and influence prostate cell proliferation. *Prostate* **66**, 326–333.

[27] Kurai M, Shiozawa T, Shih HC, Miyamoto T, Feng YZ, Kashima H, Suzuki A, and Konishi I (2005). Expression of Aurora kinases A and B in normal, hyperplastic, and malignant human endometrium: Aurora B as a predictor for poor prognosis in endometrial carcinoma. *Hum Pathol* **36**, 1281–1288.

[28] Midorikawa Y, Tsutsumi S, Nishimura K, Kamimura N, Kano M, Sakamoto H, Makuuchi M, and Aburatani H (2004). Distinct chromosomal bias of gene expression signatures in the progression of hepatocellular carcinoma. *Cancer Res* **64**, 7263–7270.

[29] Baudis M (2007). Genomic imbalances in 5918 malignant epithelial tumors: an explorative meta-analysis of chromosomal CGH data. *BMC Cancer* **7**, 226.

[30] PHA-739358 for treatment of hormone refractory prostate cancer. ClinicalTrials. gov Identifier: NCT00766324. 2007.

[31] PHA-739358 in treating patients with chronic myelogenous leukemia that relapsed after imatinib mesylate or c-ABL therapy. ClinicalTrials.gov Identifier: NCT00335868. 2007.

[32] Jackson PE, Qian GS, Friesen MD, Zhu YR, Lu P, Wang JB, Wu Y, Kensler TW, Vogelstein B, and Groopman JD (2001). Specific p53 mutations detected in plasma and tumors of hepatocellular carcinoma patients by electrospray ionization mass spectrometry. *Cancer Res* **61**, 33–35.

[33] Tannapfel A, Busse C, Weinans L, Benicke M, Katalinic A, Geissler F, Hauss J, and Wittekind C (2001). INK4a-ARF alterations and p53 mutations in hepatocellular carcinomas. *Oncogene* **20**, 7104–7109.

[34] Vogel C, Hager C, and Bastians H (2007). Mechanisms of mitotic cell death induced by chemotherapy-mediated G2 checkpoint abrogation. *Cancer Res* **67**, 339–345.

[35] Liu Q, Kaneko S, Yang L, Feldman RI, Nicosia SV, Chen J, and Cheng JQ (2004). Aurora-A abrogation of p53 DNA binding and transactivation activity by phosphorylation of serine 215. *J Biol Chem* **279**, 52175–52182.

[36] Mao JH, Wu D, Perez-Losada J, Jiang T, Li Q, Neve RM, Gray JW, Cai WW, and Balmain A (2007). Crosstalk between Aurora-A and p53: frequent deletion or downregulation of Aurora-A in tumors from p53 null mice. *Cancer Cell* **11**, 161–173.

[37] Paquette R, Shah N, Sawyers CL, Martinelli G, John N, Chalukya M, Rocchetti M, Fiocchi C, Comis S, Capolongo L, et al. (2007). PHA-739358, an Aurora kinase inhibitor, induces clinical responses in chronic myeloid leukemia harboring T315I mutations of BCR-ABL. *Blood* **110** (11, Pt 1); Abstract no. 1030.

[38] Koike K, Takaki A, Tatsukawa M, Suzuki M, Shiraha H, Iwasaki Y, Sakaguchi K, and Shiratori Y (2006). Combination of 5-FU and IFNα enhances IFN signaling pathway and caspase-8 activity, resulting in marked apoptosis in hepatoma cell lines. *Int J Oncol* **29**, 1253–1261.

[39] Saxena NK, Sharma D, Ding X, Lin S, Marra F, Merlin D, and Anania FA (2007). Concomitant activation of the JAK/STAT, PI3K/AKT, and ERK signaling is involved in leptin-mediated promotion of invasion and migration of hepatocellular carcinoma cells. *Cancer Res* **67**, 2497–2507.

[40] Yang H, He L, Kruk P, Nicosia SV, and Cheng JQ (2006). Aurora-A induces cell survival and chemoresistance by activation of Akt through a p53-dependent manner in ovarian cancer cells. *Int J Cancer* **119**, 2304–2312.

[41] Hsu IC, Tokiwa T, Bennett W, Metcalf RA, Welsh JA, Sun T, and Harris CC (1993). p53 gene mutation and integrated hepatitis B viral DNA sequences in human liver cancer cell lines. *Carcinogenesis* **14**, 987–992.

[42] Puisieux A, Galvin K, Troalen F, Bressac B, Marcais C, Galun E, Ponchel F, Yakicier C, Ji J, and Ozturk M (1993). Retinoblastoma and p53 tumor suppressor genes in human hepatoma cell lines. *FASEB J* **7**, 1407–1413.

[43] Plentz RR, Park YN, Lechel A, Kim H, Nellessen F, Langkopf BH, Wilkens L, Destro A, Fiamengo B, Manns MP, et al. (2007). Telomere shortening and inactivation of cell cycle checkpoints characterize human hepatocarcinogenesis. *Hepatology* **45**, 968–976.

[44] Willenbring H, Sharma AD, Vogel A, Lee AY, Rothfuss A, Wang Z, Finegold M, and Grompe M (2008). Loss of p21 permits carcinogenesis from chronically damaged liver and kidney epithelial cells despite unchecked apoptosis. *Cancer Cell* **14**, 59–67.

[45] Dar AA, Belkhiri A, Ecsedy J, Zaika A, and El-Rifai W (2008). Aurora kinase A inhibition leads to p73-dependent apoptosis in p53-deficient cancer cells. *Cancer Res* **68**, 8998–9004.

[46] Gizatullin F, Yao Y, Kung V, Harding MW, Loda M, and Shapiro GI (2006). The Aurora kinase inhibitor VX-680 induces endoreduplication and apoptosis preferentially in cells with compromised p53-dependent postmitotic checkpoint function. *Cancer Res* **66**, 7668–7677.

[47] Yuan RH, Jeng YM, Chen HL, Lai PL, Pan HW, Hsieh FJ, Lin CY, Lee PH, and Hsu HC (2006). Stathmin overexpression cooperates with p53 mutation and osteopontin overexpression, and is associated with tumour progression, early recurrence, and poor prognosis in hepatocellular carcinoma. *J Pathol* **209**, 549–558.

[48] Villanueva A, Chiang DY, Newell P, Peix J, Thung S, Alsinet C, Tovar V, Roayaie S, Minguez B, Sole M, et al. (2008). Pivotal role of mTOR signaling in hepatocellular carcinoma. *Gastroenterology* **135** (6), 1972–1983; 1983.e1–e11.